

Higher-order interactions in complex networks of phase oscillators promote abrupt synchronization switching

Per Sebastian Skardal*¹ and Alex Arenas²

¹Department of Mathematics, Trinity College, Hartford, CT 06106, USA

²Department d'Enginyeria Informàtica i Matemàtiques, Universitat Rovira i Virgili, 43007
Tarragona, Spain

Synchronization dynamics of network-coupled oscillators represents an important area of research in nonlinear science and complex networks [1, 2]. Applications where synchronization plays a critical role in a system's functionality include cardiac rhythms [3], power grid dynamics [4], and proper cell circuit behavior [5]. The interplay between structure and dynamics in such systems gives rise to novel nonlinear phenomena like switch-like abrupt transitions to synchronization [6, 7, 8] and cluster states [9, 10]. Recent work in physics and neuroscience have specifically highlighted the importance of higher-order interactions between dynamical units, i.e., three- and four-way interactions in addition to pair-wise interactions, and their role in shaping collective behavior [11, 12, 13, 14, 15, 16, 17, 18]. Here we show that higher-order interactions between coupled phase oscillators, encoded microscopically in a simplicial complex [19], give rise to added nonlinearity in the macroscopic system dynamics that induces abrupt synchronization transitions via hysteresis and bistability of synchronized and incoherent states. Moreover, these higher-order interactions can stabilize strongly synchronized states even when the pairwise coupling is repulsive. These findings reveal a self-organized phenomenon that may be responsible for the rapid switching to synchronization in many biological systems, without the need of particular correlation mechanisms between the oscillators and the topological structure.

*Electronic address: persebastian.skardal@trincoll.edu

The collective dynamics of network-coupled dynamical systems has been a major subject of research in the physics community during the last decades. In particular, our understanding of both natural and man-made systems has significantly improved by studying how network structures and dynamical processes combine shape overall system behaviors. Recently, the network science community has turned its attention to simplicial geometry to better represent the kinds of interactions that one can find beyond typical pairwise interactions [20]. These higher-order interactions are encoded in simplicial complexes [19] that describe the different kinds of simplex structure present in the network: a filled clique of $m + 1$ nodes is known as an m -simplex, and together a set of 1-simplexes (links), 2-simplexes (filled triangles), etc. comprise the simplicial complex. While simplicial complexes have been proven to be very useful for analysis and computation in high dimensional data sets, e.g., using persistent homologies [15], little is understood about their role in shaping dynamical processes, save for a handful of examples [21, 22].

Using brain dynamics as a motivating application, we study the dynamics of heterogeneous phase oscillators with higher-order interactions on simplicial complexes with 1-, 2-, and 3-simplex interactions. (Note that neuronal-like integrate-and-fire and can be mapped to phase oscillators [23]). For a simplicial complex of N nodes we consider an extension of the network Kuramoto model [24] whose equations of motion are given by

$$\begin{aligned} \dot{\theta}_i = & \omega_i + \frac{K_1}{\langle k^1 \rangle} \sum_{j=1}^N A_{ij} \sin(\theta_j - \theta_i) + \frac{K_2}{2\langle k^2 \rangle} \sum_{j=1}^N \sum_{l=1}^N B_{ijl} \sin(2\theta_j - \theta_l - \theta_i) \\ & + \frac{K_3}{6\langle k^3 \rangle} \sum_{j=1}^N \sum_{l=1}^N \sum_{m=1}^N C_{ijlm} \sin(\theta_j + \theta_l - \theta_m - \theta_i), \end{aligned} \quad (1)$$

where θ_i is the phase of oscillator i , ω_i is its natural frequency (typically assumed to be drawn from a distribution $g(\omega)$), and K_1 , K_2 , and K_3 are the coupling strengths of 1-, 2-, and 3-simplex interactions, respectively. The network structure (assumed to be undirected and unweighted) is encoded in the 1-simplex adjacency matrix A , 2-simplex adjacency tensor B , and 3-simplex adjacency tensor C , where $A_{ij} = 1$ if nodes i and j are connected by a link (and otherwise $A_{ij} = 0$), $B_{ijl} = 1$ if nodes i , j , and l belong to a common 2-simplex (and otherwise $B_{ijl} = 0$), and $C_{ijlm} = 1$ if nodes i , j , l , and m belong to a common 3-simplex (and otherwise $C_{ijlm} = 0$). For each node i we denote the q -simplex degree k_i^q as the number of distinct q -simplexes node i is a part of, and $\langle k^q \rangle$ is the mean q -simplex degree across the network. (Note that each division by $\langle k^q \rangle$ in equation (1) amounts to a rescaling of the respective coupling strength).

Taking inspiration from the importance of simplicial complexes in the brain, which displays rich synchronization dynamics [25], we consider as a motivating example the dynamics of equation (1) on the Macaque brain dataset which consists of 242 interconnected regions of the brain [26]. The adjacency matrix A is taken to be undirected and 2- and 3-simplex structures are constructed

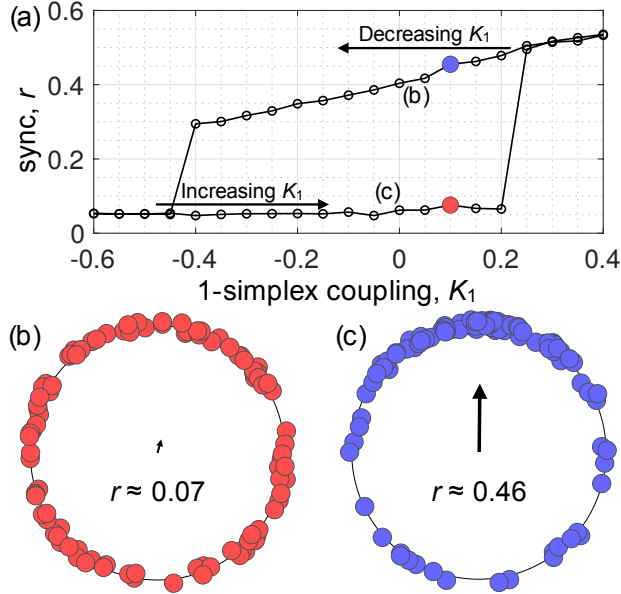


Figure 1: **Abrupt synchronization in simplicial complexes: Macaque brain dataset.** (a) The synchronization profile describing the macroscopic system state by the order parameter r as a function of 1-simplex coupling K_1 for higher-order coupling strengths $K_2 = 1.6$ and $K_3 = 1.1$. Results are obtained by adiabatically increasing K_1 from -0.6 to 0.4 , then subsequently decreasing K_1 from 0.4 back to -0.6 . This protocol reveals a hysteresis loop with abrupt synchronization and desynchronization transitions at $K_1^{\text{sync}} \approx 0.25$ and $K_1^{\text{desync}} \approx -0.4$ with a bistable region of incoherence and synchronization in between. Incoherent and synchronized states at $K_1 = 0.1$ are illustrated in panels (b) and (c), respectively.

by identifying each distinct triangle and tetrahedron from the 1-simplex structures. The 2- and 3-simplex coupling strengths are fixed to $K_2 = 1.6$ and $K_3 = 1.1$ as the 1-simplex coupling strength is varied and natural frequencies are drawn identically and independently from the standard normal distribution. In Fig. 1(a) we plot the amplitude r of the complex order parameter $z = r e^{i\psi} = N^{-1} \sum_{j=1}^N e^{i\theta_j}$ as K_1 is first increased adiabatically from $K_1 = -0.6$ to 0.4 , then decreased. These simulations reveal that the presence of higher-order interactions in simplicial complexes give rise to abrupt (a.k.a. explosive) synchronization transitions [6], as the system quickly transitions from the incoherent state ($r \approx 0$) to a partially synchronized state ($r \sim 1$) at $K_1^{\text{sync}} \approx 0.25$ as K_1 is increased, then another abrupt transition from synchronization to incoherence occurs at $K_1^{\text{desync}} \approx -0.4$ as K_1 is decreased. For $K_1 \in [K_1^{\text{desync}}, K_1^{\text{sync}}]$ the system admits a bistability where both incoherent and synchronized states are stable. In Figs. 1(b) and (c) we highlight this bistability by showing the incoherent and synchronized states, respectively, for $K_1 = 0.1$, illustrating for 40% of the oscillators (chosen randomly) placed appropriately on the unit circle with their respective order parameter values $r \approx 0.07$ and 0.46 .

The results presented above illustrate two new critical findings using a real brain dataset. First, the presence of higher-order interactions, i.e., 2- and 3-simplexes, can induce abrupt synchronization transitions without any additional dynamical or structural ingredients. Incoherent and synchronized

states have been mapped to resting and active states of the brain [27], respectively, with abrupt transitions representing quick and efficient mechanisms for switching cognitive tasks. However, previous work has shown that in the presence of only 1-simplex coupling, properties such as time-delays [28] or degree-frequency correlations [6] are needed to induce such transitions. Second, the presence of higher-order interactions can create and stabilize a synchronized state even when 1-simplex coupling is negative, i.e., repulsive. Thus, higher-order interactions nonlinear effects that support synchronization on the macroscopic scale.

To better understand the dynamics that emerge in the system above, we turn our focus to a population of all-to-all coupled oscillators. The governing equations, which also serves as the mean-field approximation for equation (1), is given by

$$\begin{aligned} \dot{\theta}_i = \omega_i + \frac{K_1}{N} \sum_{j=1}^N \sin(\theta_j - \theta_i) + \frac{K_2}{N^2} \sum_{j=1}^N \sum_{l=1}^N \sin(2\theta_j - \theta_l - \theta_i) \\ + \frac{K_3}{N^3} \sum_{j=1}^N \sum_{l=1}^N \sum_{m=1}^N \sin(\theta_j + \theta_l - \theta_m - \theta_i). \end{aligned} \quad (2)$$

In the all-to-all case given by equation (2) the system can be treated using the dimensionality reduction of Ott and Antonsen [29], yielding a low dimensional system that governs the macroscopic dynamics via the order parameter $z = r e^{i\psi}$. In particular, by considering the continuum limit of infinitely-many oscillators and applying the Ott-Antonsen ansatz (see Methods for details), we obtain for the amplitude r and angle ψ the simple differential equations

$$\dot{r} = -r + \frac{K_1}{2} r(1 - r^2) + \frac{K_{2+3}}{2} r^3(1 - r^2), \quad (3)$$

$$\dot{\psi} = \omega_0, \quad (4)$$

where we have assumed that the natural frequency distribution $g(\omega)$ is Lorentzian with mean ω_0 and the new coupling strength is given by the sum of the 2- and 3-simplex coupling strengths, i.e., $K_{2+3} = K_2 + K_3$. Note first that the amplitude and angle dynamics of r and ψ completely decouple and that the angle dynamics evolve with a constant angular velocity equal to the mean of the frequency distribution. Thus, by entering an appropriate rotating frame and shifting initial conditions we may set $\psi = 0$ without any loss of generality. Moreover, the higher-order interactions, i.e., 2- and 3-simplexes mediated by the coupling strength K_{2+3} , surface in the form of cubic and quintic nonlinear terms. This implies that the stability of the incoherent state, given by $r = 0$, (which is always an equilibrium) is not affected by the higher-order interactions. However, these nonlinear terms that originate from the higher-order interactions mediate the possibility of

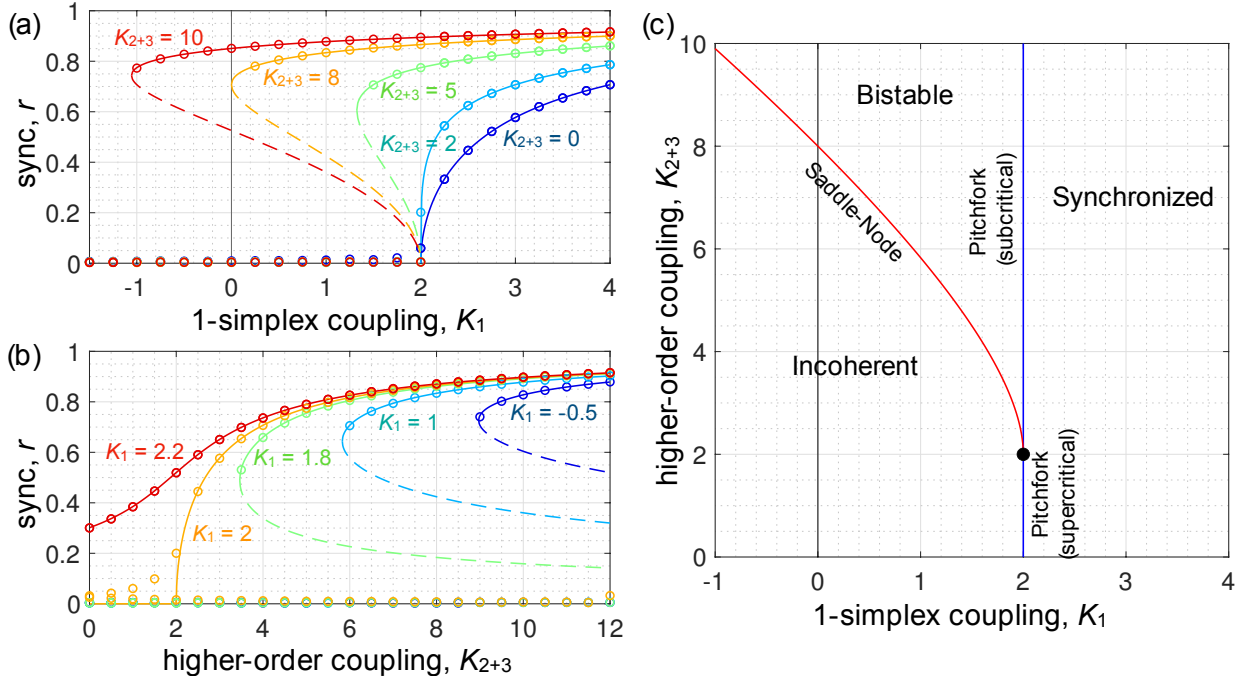


Figure 2: **Abrupt synchronization in simplicial complexes: All-to-all case.** Synchronization profiles describing the macroscopic system state: (a) the order parameter r as a function of 1-simplex coupling K_1 for higher-order coupling $K_{2+3} = 0, 2, 5, 8,$ and 10 (blue to red) and (b) the order parameter r as a function of higher-order coupling K_{2+3} for 1-simplex coupling $K_1 = -0.5, 1, 1.8, 2,$ and 2.2 . Solid and dashed curves represent stable and unstable solutions given by equation (5), respectively, and circles denote results taken from direct simulations of equation (2) with $N = 10^4$ oscillators. (c) The full stability diagram describing incoherent, synchronized, and bistable states as a function of 1-simplex coupling K_1 and higher-order coupling K_{2+3} . Blue and red curves correspond to pitchfork and saddle-node bifurcations, which collide at a codimension-two point (black circle) at $(K_1, K_{2+3}) = (2, 2)$. For $K_{2+3} < 2$ and $K_{2+3} > 2$ the pitchfork bifurcation is supercritical and subcritical, respectively.

synchronized states. In particular, one or two synchronized states also exists, given by

$$r = \sqrt{\frac{K_{2+3} - K_1 \pm \sqrt{(K_1 + K_{2+3})^2 - 8K_{2+3}}}{2K_{2+3}}}, \quad (5)$$

where the plus and minus signs correspond to stable and unstable solutions when they exist.

We now show that the all-to-all case illustrates, in an analytically tractable setting, all the novel dynamics observed in the Macaque example (see Fig. 1). First, in Fig. 2(a) we plot steady-state solutions of the order parameter r as a function of the 1-simplex coupling strength K_1 for a variety of higher-order coupling strengths $K_{2+3} = 0, 2, 5, 8,$ and 10 (blue to red). Analytical predictions given by equation 5 are plotted as solid and dashed curves (for stable and unstable branches, respectively), and circles represent results from direct simulation of equation (1) with $N = 10^4$ oscillators. For sufficiently small higher-order coupling (e.g., $K_{2+3} = 0$) the transition to synchronization is second-

order, occurring via a supercritical pitchfork bifurcation. However, as K_{2+3} is increased through a critical value of $K_1^{\text{sync}} = 2$ the synchronized branch folds over itself, giving rise to hysteresis and abrupt transitions between incoherence and synchronization for larger values of higher-order coupling (e.g., $K_{2+3} = 5, 8,$ and 10). In this regime the pitchfork bifurcation at $K_1^{\text{sync}} = 2$ becomes subcritical and a saddle-node bifurcation emerges at a lower value of K_1 , denoted K_1^{desync} , where the synchronized branch first appears. These two bifurcations correspond to the abrupt transitions observed in Fig. 1. We also observe that for $K_{2+3} \geq 8$ the synchronized branch stretches into the negative region $K_1 < 0$ (e.g., $K_{2+3} = 10$), again demonstrating that higher-order interactions can stabilize synchronized states even when pairwise interactions are repulsive. In Fig. 2(b) we plot similar results as the higher-order coupling strength K_{2+3} is varied for a variety of 1-simplex coupling strengths, $K_1 = -0.5, 1, 1.8, 2,$ and 2.2 (blue to red). These curves highlight the existence and absence of bistability for $K_1 < 2$ and $K_1 > 2$, respectively. In Fig. 2(c) we provide the full stability diagram for the system, denoting the pitchfork bifurcations at $K_1^{\text{sync}} = 2$ (supercritical and subcritical for $K_{2+3} < 2$ and $K_{2+3} > 3$) in blue and the saddle-node bifurcation, given by $K_1^{\text{desync}} = 2\sqrt{2K_{2+3}} - K_{2+3}$, in red. The region bounded by these curves corresponds to bistability between synchronization and incoherence, and is born at the intersection between the two bifurcations at the codimension-two point $(K_1, K_{2+3}) = (2, 2)$.

Having demonstrated the novel synchronization dynamics that arise from higher-order interactions in simplicial complexes in a real brain dataset and the all-to-all scenario, we lastly turn to a synthetic network example, constructing a simplicial complex via a three-layer multiplex, where the q^{th} layer consists of q -simplexes. In particular, aiming for such a multiplex with mean degrees $\langle k^1 \rangle$, $\langle k^2 \rangle$, and $\langle k^3 \rangle$, we construct each layer randomly, placing $M_1 = N\langle k^1 \rangle/2$ 1-simplexes (i.e., links) in the first layer, $M_2 = N\langle k^2 \rangle/3$ 2-simplexes (i.e., filled triangles) in the second layer, and $M_3 = N\langle k^3 \rangle/4$ 3-simplexes (i.e., filled tetrahedra) in the third layer. (Note that the first layer is a classical Erdős-Rényi network [30] and the second and third layers are the generic extensions using 2- and 3-simplexes instead of typical links.) In Figs. 3(a) and (b) we plot the the order parameter r vs 1-simplex coupling K_1 and higher-order coupling K_{2+3} , respectively, for a multiplex network of $N = 10^4$ oscillators with mean degrees $\langle k^1 \rangle = \langle k^2 \rangle = \langle k^3 \rangle = 30$ in circles. Similar to Figs. 2(a) and (b), solid and dashed curves represent the analytical results for the mean-field approximation from the all-to-all case. These results illustrate that the mean-field approximation accurately describes the dynamics of such randomly generated simplicial complexes.

The results presented above demonstrate that higher-order interactions in networks of coupled oscillators, which are encoded on the microscopic scale of by a simplicial complex, give rise to added nonlinearities in the macroscopic system dynamics. These nonlinearities give rise to two new phenomena that are not present in the absence of higher-order interactions, i.e., when interactions are solely pairwise. First, these nonlinearities induce abrupt transitions between incoherent and synchronized states without additional characteristics such as time delays or network-dynamics

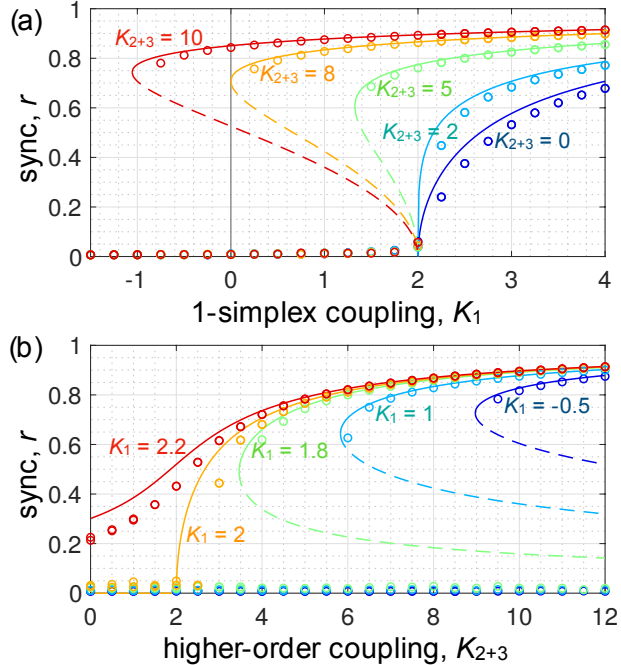


Figure 3: **Synchronization in the multiplex simplicial complex model.** For the multiplex model of simplicial complexes, synchronization profiles describing the macroscopic system state: (a) the order parameter r as a function of 1-simplex coupling K_1 for higher-order coupling $K_{2+3} = 0, 2, 5, 8,$ and 10 (blue to red) and (b) the order parameter r as a function of higher-order coupling K_{2+3} for 1-simplex coupling $K_1 = -0.5, 1, 1.8, 2,$ and 2.2 . Circles represent direct simulations on a network of $N = 10^4$ nodes with mean degrees $\langle k^1 \rangle = \langle k^2 \rangle = \langle k^3 \rangle = 30$ and solid and dashed curves represent stable and unstable solutions of the mean field approximation given by equation (5).

correlations. In the context of brain dynamics, incoherent and synchronized states correspond to resting and active states, with abrupt transitions facilitating efficient switching between cognitive tasks [27]. Second, when nonlinearities are sufficiently strong they create and stabilize synchronized states even when pair-wise coupling is repulsive. Thus, even as certain kinds of coupling may degrade over time due to synaptic plasticity, the presence of other kinds of coupling may be enough to sustain bistability regimes between incoherence and synchronization. We note that in this Letter we have taken brain dynamics as our primary motivating example due to the existence of direct evidence of higher-order interactions in a system with synchronization properties [11, 12, 14, 17]. However, more general results suggest that higher-order interactions may be important in broader classes of physical systems [13, 18], indicating that the nonlinear phenomena observed in this context may point to other novel behaviors that arise from such interactions in different contexts.

Methods

Here we detail the dimensionality reduction used to derive equations (2) and (3). We begin by rewriting equation (1) using the complex order parameters z and z_2 , yielding

$$\dot{\theta}_i = \omega_i + \frac{1}{2i} \left(H e^{-i\theta_i} - H^* e^{i\theta_i} \right), \quad (6)$$

where $H = K_1 z + K_2 z_2 z_1^* + K_3 z_1^2 z_1^*$ and $*$ denotes the complex conjugate. In the thermodynamic limit we may represent the state of the system using the density function $f(\theta, \omega, t)$, where $f(\theta, \omega, t) d\theta d\omega$ gives the fraction of oscillator with phase in $[\theta, \theta + d\theta)$ and frequency in $[\omega, \omega + d\omega)$ at time t . Because oscillators are conserved and frequencies are fixed, f satisfies the continuity equation

$$0 = \frac{\partial f}{\partial t} + \frac{\partial}{\partial \theta} \left\{ f \left[\omega_i + \frac{1}{2i} \left(H e^{-i\theta_i} - H^* e^{i\theta_i} \right) \right] \right\}. \quad (7)$$

Expanding f into its Fourier series $f(\theta, \omega, t) = \frac{g(\omega)}{2\pi} \left[1 + \sum_{n=1}^{\infty} \hat{f}_n(\omega, t) e^{in\theta} + \text{c.c.} \right]$ (where c.c. denoted the complex conjugate of the previous term), we follow Ott and Antonsen [29] and ansatz that Fourier coefficients decay geometrically, i.e., $\hat{f}_n(\omega, t) = \alpha^n(\omega, t)$ for some function α that is analytic in the complex ω plane. Remarkably, after inserting this ansatz into f and f into equation (7), all Fourier modes collapse onto the same constraint for α , giving the single differential equation

$$\dot{\alpha} = -i\omega\alpha + \frac{1}{2} (H^* - H\alpha^2). \quad (8)$$

Moreover, in the thermodynamic limit we have that $z^* = \iint f(\theta, \omega, t) e^{i\theta} d\theta d\omega = \int \alpha(\omega, t) g(\omega) d\omega$. By letting g be Lorentzian with mean ω_0 and width Δ , i.e., $g(\omega) = \Delta/\pi[\Delta^2 + (\omega - \omega_0)^2]$, this integral can be evaluated by closing the contour with the infinite-radius semi-circle in the negative-half complex plane and using Cauchy's integral theorem [31], yielding $z^* = \alpha(\omega_0 - i\Delta, t)$. (Similarly, we have that $z_2^* = \alpha^2(\omega_0 - i\Delta) = z^{*2}$.) Evaluating equation (8) at $\omega = \omega_0 - i\Delta$ and taking a complex conjugate then yields

$$\dot{z} = -\Delta z + i\omega_0 z + \frac{1}{2} \left[(K_1 z + K_{2+3} z^2 z^*) - (K_1 z^* + K_{2+3} z^{*2} z) z^2 \right]. \quad (9)$$

Using the rescaled time $\hat{t} = \delta t$ and rescaled coupling strengths $\hat{K}_1 = K_1/\Delta$ and $\hat{K}_{2+3} = K_{2+3}/\Delta$ (effectively setting $\Delta = 1$) and separating equation (9) into evolution equations for r and ψ yields (after dropping the \wedge -notation) equations (2) and (3).

References

- [1] S. H. Strogatz, *Sync: the Emerging Science of Spontaneous Order* (Hyperion, 2003).
- [2] A. Arenas, A. Díaz-Guilera, J. Kurths, Y. Moreno, C. Zhou, Synchronization in complex networks. *Phys. Rep.* **469**, 93–153 (2008).
- [3] A. Karma, Physics of cardiac arrhythmogenesis. *Annu. Rev. Condens. Matter Phys.* **4**, 313–337 (2013).
- [4] M. Rohden, A. Sorge, M. Timme, D. Witthaut, Self-organized synchronization in decentralized power grids. *Phys. Rev. Lett.* **109**, 064101 (2012).
- [5] A. Prindle, P. Samayoa, I. Razinkov, T. Danino, L. S. Tsimring, J. Hasty, A sensing array of radically coupled genetic ‘biopixels’. *Nature* **481**, 39–44 (2011).
- [6] J. Gómez-Gardeñes, S. Gómez, A. Arenas, Y. Moreno, Explosive synchronization transitions in scale-free networks. *Phys. Rev. Lett.* **106**, 128701 (2011).
- [7] P. S. Skardal, A. Arenas, Abrupt desynchronization and extensive multistability in globally coupled oscillator simplexes. *Phys. Rev. Lett.* **122**, 248301 (2019).
- [8] R. D’Souza, J. Gómez-Gardeñes, J. Nagler and A. Arenas, Explosive phenomena in complex networks, *Advances in Physics*, **68**, 123-223 (2019).
- [9] L. M. Pecora, F. Sorrentino, A. M. Hagerstrom, T. E. Murphy, R. Roy, Cluster synchronization and isolated desynchronization in complex networks with symmetries. *Nat. Commun.* **5**, 4079 (2014).
- [10] Y. S. Cho, T. Nishikawa, A. E. Motter, Stable chimeras and independently synchronizable clusters. *Phys. Rev. Lett.* **119**, 084101 (2017).
- [11] G. Petri, P. Expert, F. Turkheimer, R. Carhart-Harris, D. Nutt, P.J. Hellyer, F. Vaccarino, Homological scaffolds of brain functional networks, *J. R. Soc. Interface* **11**, 20140873 (2014).
- [12] C. Giusti, R. Ghrist, D. S. Bassett, Two’s company, three (or more) is a simplex, *J. Comput. Neurosci.* **41**, 1 (2016).
- [13] P. Ashwin, A. Rodrigues, Hopf normal form with S_N symmetry and reduction to systems of nonlinearly coupled phase oscillators, *Physica D* **325**, 14 (2016).
- [14] M. W. Reimann, M. Nolte, M. Scolamiero, K. Turner, R. Perin, G. Chindemi, P. Dlotko, R. Levi, K. Hess, H. Markram, Cliques of neurons bound into cavities provide a missing link between structure and function, *Frontiers in Comp. Neuro.* **11**, 48 (2017).

- [15] N. Otter, M. A. Porter, U. Tillman, P. Grindrod, and H. A. Harrington, A roadmap for the computation of persistent homology, *Euro. Phys. J. DS* **6**, 17 (2017).
- [16] A. P. Millán, J. Torres and G. Bianconi, Complex network geometry and frustrated synchronization, *Scientific Reports* **1**, 9910 (2018).
- [17] A. E. Sizemore, C. Giusti, A. Kahn, J. M. Vettel, R. Betzel, D. S. Bassett, Cliques and cavities in the human connectome, *J. Comput. Neurosci.* **44**, 115 (2018).
- [18] I. León, D. Pazó, Phase reduction beyond the first order: The case of the mean-field complex Ginzburg-Landau equation. *Phys. Rev. E* **100**, 012211 (2019).
- [19] V. Salnikov, D. Cassese, R. Lambiotte, Simplicial complexes and complex systems. *Eur. J. Phys.* **40**, 014001 (2019).
- [20] D. Horak, S. Maletić and M. Rajković, Persistent homology of complex networks, *J. of Stat. Mech.* **3**, P03034 (2009).
- [21] I. Iacopini, G. Petri, A. Barrat, V. Latora, Simplicial models of social contagion. *Nat. Commun.* **10**, 2485 (2019).
- [22] M. T. Schaub, A. R. Benson, P. Horn, G. Lippner, A. Jadbabaie, Random walks on simplicial complexes and the normalized Hodge-1 Laplacian. arXiv:1807.05044.
- [23] A. Politi, and M. Rosenblum, Equivalence of phase-oscillator and integrate-and-fire models. *Phys. Rev. E* **91**, 4, 042916 (2015).
- [24] Y. Kuramoto, *Chemical Oscillations, Waves, and Turbulence* (Springer, New York, 1984).
- [25] A. Schnitzler, J. Gross, Normal and pathological oscillatory communication in the brain. *Nat. Rev. Neurosci.* **6**, 285–296 (2005).
- [26] K. Amunts, C. Lepage, L. Borgeat, H. Mohlberg, T. Dickscheid, M.-E. Rousseau, S. Bludau, P.-L. Bazin, L. B. Lewis, A. M. Oros-Peusquens, N. J. Shah, T. Lippert, K. Zilles, A. C. Evans, BigBrain: An ultrahigh-resolution 3D human brain model. *Science* **340**, 1472–1475 (2013).
- [27] G. Deco, V. K. Jirsa, A. R. McIntosh, resting brains never rest: Computational insights into potential cognitive architectures. *Trends Neurosci.* **36**, 268–274 (2013).
- [28] W. S. Lee, E. Ott, and T. M. Antonsen, Large coupled oscillator systems with heterogeneous interaction delays. *Phys. Rev. Lett.* **103**, 044101.
- [29] E. Ott, T. M. Antonsen, Low dimensional behavior of large systems of globally coupled oscillators. *Chaos* **18**, 037113 (2008).

- [30] P. Erdős, A. Rényi, On the evolution of random graphs. *Publ. Math. Inst. Hung. Acad. Sci.* **5**, 17–61 (1960).
- [31] M. J. Ablowitz, A. S. Fokas, *Complex Variables: Introduction and Applications* (Cambridge University Press, 2003).

Acknowledgements

AA acknowledges support by Ministerio de Economía y Competitividad (Grants No. PGC2018-094754-B-C21 and No. FIS2015-71929-REDT), Generalitat de Catalunya (Grant No. 2017SGR-896), and Universitat Rovira i Virgili (Grant No. 2017PFR-URV-B2-41), ICREA Academia and the James S. McDonnell Foundation (Grant No. 220020325).

Author Contributions

PSS and AA conceived the study. PSS performed the analytical calculations, numerical experiments, and analyzed the results. PSS and AA wrote the manuscript.

Competing Interests

The authors declare that they have no competing interests.